Functional Nanogels as Platforms for Imparting Antibacterial, Antibiofilm, and Antiadhesion Activities to Stainless Steel

*Emilie Faure, Céline Falentin-Daudré, Tiziana Svaldo Lanero, Christelle Vreuls, Germaine Zocchi, Cécile Van De Weerdt, Joseph Martial, Christine Jérôme, Anne-Sophie Duwez, and Christophe Detrembleur**

In this work, long-term antibacterial, antiadhesion, and antibiofilm activities are afforded to industrial stainless steel surfaces following a green and bio-inspired strategy. Starting from catechol bearing synthetic polymers, the film cross-linking and the grafting of active (bio)molecules are possible under environmentally friendly conditions (in aqueous media and at room temperature). A bio-inspired polyelectrolyte, a polycation-bearing catechol, is used as the film-anchoring polymer while a poly(methacrylamide)-bearing quinone groups serves as the cross-linking agent in combination with a polymer bearing primary amine groups. The amine/quinone reaction is exploited to prepare stable solutions of nanogels in water at room temperature that can be easily deposited to stainless steel. This coating provides quinone-functionalized surfaces that are then used to covalently anchor active (bio) molecules (antibiofilm enzyme and antiadhesion polymer) through thiol/quinone reactions.

1. Introduction

Layer-by-layer (LbL) technology has been widely developed in the literature during last decades because of its simplicity and versatility in coating every kind and shape of substrates.[1] Many scientific reviews based on multilayers films built by electrostatic interactions[2] or hydrogen bonds[3] were published during the last ten years traducing the growing interest in this technique. However these building strategies have one major drawback: the lack of long-term durability. Therefore covalent assembly is particularly attractive to overcome this limitation and has demonstrated to have huge potential in the coating field.[4] Considering the cross-linking growth from aqueous solutions, covalent coupling can be afforded by physical (UV[5] or thermal[6] curing) or chemical post-treatments. In the latter case, complementary reactive groups are present on the two polyelectrolytes partners that are involved in the multilayer film. These groups are for instances amine (or alcohol) with carboxylic acid groups,[7] with aldehydes[8] or epoxides.[9] Click chemistry has also been applied to cross-link multilayers films.[10] All these cross-linking strategies therefore require a post-treatment of the LbL film that increases the cost and time needed to get the substrate fully functionalized. Strategies involving two components that cross-link together during the film building without post-treatment exist but demand long immersion times.[11]

We report here on a fast and water based cross-linking process exploiting the redox properties of DOPA molecules to provide reactive coatings available for further modifications in mild conditions. We tailored a homopolymer of methacrylamide bearing 3,4-dihydroxy-L-phenylalanine (P(mDOPA), **1**, **Figure 1**) specifically designed to covalently cross-link the multilayer film during the building process and to covalently immobilize active (bio)molecules. This strategy has several advantages over existing methods: i) it is a one step procedure without further purification or post-treatment, ii) there is no use of external cross-linking agent, iii) coupling reactions are fast at room temperature in water, iv) no undesirable side products are formed and released out of the film, and v) active (bio)molecules can be covalently grafted to the surface. Furthermore, for the first time, we will report on novel water-based cross-linked reactive nanogels that can be directly deposited onto the surface pre-coated by a bio-inspired glue, a cationic polyelectrolyte bearing DOPA units (P(mDOPA)-*co*-P(DMAEMA$^+$), **4**, Figure 1)[12] that mimics the composition of adhesive proteins present in mussel foot.[13] Fast substrate functionalization is therefore now available using environmentally friendly procedures. The efficiency and versatility of the two strategies investigated in this paper will be illustrated by

Dr. E. Faure, Dr. C. Falentin-Daudré, Prof. C. Jérôme, Dr. C. Detrembleur
Center for Education and Research on Macromolecules
University of Liège
B6, Sart Tilman, 4000 Liège, Belgium
E-mail: christophe.detrembleur@ulg.ac.be
Dr. T. Svaldo Lanero, Prof. A.-S. Duwez
Nanochemistry and Molecular Systems
University of Liège
B6, Sart-Tilman, 4000 Liège, Belgium
Dr. C. Vreuls, Dr. G. Zocchi, Dr. C. Van De Weerdt, Prof. J. Martial
Laboratoire de Biologie Moléculaire et de Génie Génétique
GIGA-Research, CHU, B34, Sart Tilman, 4000 Liège, Belgium

DOI: 10.1002/adfm.201201106

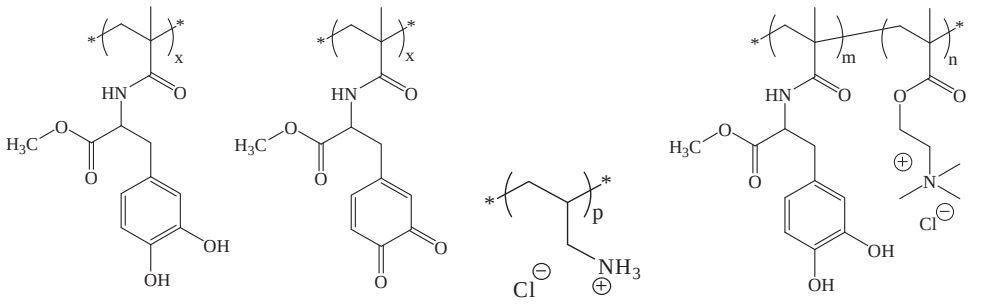

1 **2** **3** **4**

Figure 1. Chemical structures of (**1**) P(mDOPA), (**2**) Pox(mDOPA) (**3**) PAH, and (**4**) P(mDOPA)-*co*-P(DMAEMA$^+$).

imparting long-term antibacterial, antibiofilm but also antiadhesion properties to stainless steel (SS) substrates.

2. Results and Discussion

In this work, the cross-linking of the LbL film occurs through the well-known amine/quinone reactions[14] between a poly(methacrylamide) bearing quinones (oxidized DOPA moieties) on each monomer unit (Pox(mDOPA), **2**, Figure 1)[15] and a commercially available polymer containing primary amines, poly(allylamine) (PAH, **3**, Figure 1). Importantly, both partners are covalently coupled through Schiff base formation and/or Michael addition reaction at room temperature in aqueous media. In order to favor the strong anchoring of the coating on the surface (industrial SS in this study), the substrate was first immersed in an aqueous solution of the bio-inspired glue that contains the adherent catechol groups, P(mDOPA)-*co*-P(DMAEMA$^+$), prior to the deposition of the cross-linked coating.

The poly(methacrylamide) bearing DOPA units (P(mDOPA), **1**, Figure 1) is therefore used as the main platform for the preparation of the functional coating. The versatility and efficiency of the developed systems are illustrated below by designing new antibacterial and antibiofilm/antiadhesion coatings on industrial stainless steel surfaces using both the LbL and the nanogels approaches.

2.1. LbL Deposition of Silver-Loaded Polymer (Pox(mDOPA)-Ag^0) with PAH and Antibacterial Activity

Silver nitrate addition to the aqueous dispersion of **1** leads to the fast reduction by the catechol groups of Ag$^+$ into elemental silver nanoparticles (Ag^0)[12,16] that are stabilized by the water-soluble oxidized polymer (Pox(mDOPA), **2**, Figure 1). This reaction that occurs in water at room temperature imparts multifunctionality to the polymer i) by loading it with biocidal Ag^0 nanoparticles[17] and ii) by rendering it reactive towards primary amino groups and thus towards cross-linking (thanks to the quinone groups). The first strategy to design the AB coating consists in building a LbL film (see ESI, Supporting Information Figure S1) by the alternative deposition of the silver loaded polymer (Pox(mDOPA)-Ag^0) solution with PAH on stainless steel (SS) that is pre-coated by a first layer of the glue (P(mDOPA)-*co*-P(DMAEMA$^+$),[12]**4**, Figure 1). This glue is first deposited by dipping the substrate into an aqueous solution of **4** at 2 g L^{-1} at room temperature. Then the successive substrate immersions into Pox(mDOPA)-Ag^0 and PAH aqueous solutions contribute to the multilayer growth (see ESI, Supporting Information Figure S1). It is important to mention that the pH of PAH solution is adjusted to about 10 in order to get its primary amines deprotonated, and therefore having them reactive towards the quinone groups of Pox(mDOPA).

The formation of the silver nanoparticles by P(mDOPA) in aqueous solution was characterized by transmission electron microscopy (TEM) and energy-dispersive X-ray (EDX) spectroscopy. The presence of small metal particles in the 10 nanometer range for an aqueous solution of Pox(mDOPA)-Ag^0 at a concentration of 0.1 g L^{-1} has been observed by TEM (see ESI, Supporting Information Figure S2). EDX is used to probe the elemental analysis of a 5-bilayers film, P(mDOPA)-*co*-P(DMAEMA$^+$)/[(Pox(mDOPA)-Ag^0/PAH)$_5$], built on SS. Intense signals around 3 keV and 3.2 keV are characteristic of Ag^0 (see ESI, Supporting Information Figure S3) and therefore prove the presence of these particles in the multilayer film.

The film building was demonstrated by quartz crystal microbalance coupled with dissipation (QCM-D) in a previous publication[15] and ellipsometry measurement reveals that a 5-bilayers film that is not silver loaded, P(mDOPA)-*co*-P(DMAEMA$^+$)/[(Pox(mDOPA)/PAH)$_5$], has a thickness of about 9-10 nm. Analysis of silver loaded films is not possible by these techniques (large baseline fluctuations in QCMD and unknown optical values for silver nanoparticles in ellipsometry).

Antibacterial (AB) activity of the silver loaded coatings in solution against Gram negative bacteria, *Escherichia coli*, was investigated by the viable-cell counting method.[18] Some of these coatings were immersed in various media for one night at 50 °C (basic water, diluted household cleaner (hhc), hot water (50 °C), etc.) and even cleaned with a wet sponge before testing in order to evaluate the efficiency of the cross-linking reactions on the durability of the AB activity.

Bare stainless steel and the LbL coating without silver nanoparticles (P(mDOPA)-*co*-P(DMAEMA$^+$)/[(Pox(mDOPA)/PAH)$_5$]) did not present any AB activity (**Table 1**, entries **1** and **2**). The uppermost layer of the multilayer film (Pox(mDOPA) and eventually uncovered PAH) is therefore not active against bacteria. On the other hand, when the silver loaded coating formed by alternating 5 layers of Pox(mDOPA)-Ag^0 and PAH (noted

Table 1. Antibacterial activity of SS substrates covered or not by DOPA-based multilayer films against *E. coli* ($T_0 = 1.7.10^5$ cell mL^{-1}; T_0 = initial number of bacteria per mL used for the test).

Entry	Sample		1 h of contact		2 h of contact		19 h of contact	
			Cell mL^{-1} [a]	Reduction rate [%]	Cell mL^{-1} [a]	Reduction rate [%]	Cell mL^{-1} [a]	Reduction rate [%]
1	Bare SS		4.1×10^5	–	1.6×10^6	–	5.3×10^6	–
2	Multilayer[b]		5.9×10^5	–	8.7×10^5	–	1×10^6	–
3	Silver loaded-multilayer[c]	Control[c]	1.2×10^2	99.93	0	100	0	100
4		Immersed in cold water	3.4×10^4	80	4.2×10^2	99.75	5.8×10^2	99.66
5		Immersed in hot water	30	99.98	0	100	0	100
6		Immersed in diluted hhc	5.4×10^3	96.8	0	100	0	100
7		Immersed in basic medium	2.3×10^4	86.5	20	99.99	0	100
8		Mechanical test	3.2×10^4	81	40	99.97	0	100

[a] Survival number of bacteria mL^{-1}; [b] (P(mDOPA)-*co*-P(DMAEMA$^+$)/[(Pox(mDOPA)/PAH)$_5$]); [c] (P(mDOPA)-*co*-P(DMAEMA$^+$)/[(Pox(mDOPA)-Ag^0/PAH)$_5$]).

(P(mDOPA)-*co*-P(DMAEMA$^+$)/[(Pox(mDOPA)-Ag^0/PAH)$_5$]) was considered, a high AB activity was observed (Table 1, entry **3**) and was preserved even after one night of immersion in water as shown by 99.96% reduction of survival bacteria compared to bare SS (Table 1, entry **4**). In order to test the durability of the coating in various conditions, five different treatments were applied to the coating before carrying out the AB test. Importantly, this AB coating activity was boosted when the substrate was immersed in hot water (50 °C) overnight prior to testing. All bacteria were killed after two h of incubation (Table 1, entry **5**). Table 1 shows that the silver loaded coatings remained highly active whatever the surface was immersed at 50 °C in diluted hhc (Table 1, entry **6**) or basic water (Table 1, entry **7**), or was cleaned with a wet sponge after being dipped one night in hot water (Table 1, entry **8**). We assume that the temperature enhances the film cross-linking rate and consequently improves the durability of the coating. For the sake of comparison, when poly(ethylenimine) (PEI; commonly used as a first layer for the anchoring of LbL films onto various surfaces)[19] was used as the first layer instead of our bio-inspired glue (P(mDOPA)-*co*-P(DMAEMA$^+$)), the AB activity was completely lost after overnight immersions in the same conditions (diluted hhc, basic water, etc.) (data not shown). This control experiment demonstrates that our copolymer bearing DOPA moieties is necessary for anchoring the coating on the SS surface and for preserving the AB activity.

Although this surface modification is highly efficient, it requires the LbL process of about 5 bilayers that makes the strategy difficult to scale-up at industrial level. In the next section, we describe how the same polymeric partners can be pre-assembled to provide AB coating in a more practical and convenient approach.

2.2. Formation of Silver Loaded Nanogels, Pox(mDOPA)-Ag^0/PAH, Deposition Onto Stainless Steel and Antibacterial Activity

Instead of alternatively depositing Pox(mDOPA)-Ag^0 and PAH onto SS for providing a cross-linked AB film, we envisioned the formation of nanogels Pox(mDOPA)-Ag^0/PAH in aqueous solution (see ESI, Supporting Information Figure S4) prior to their deposition on the substrate that has been pre-coated by the glue (P(mDOPA)-*co*-P(DMAEMA$^+$)) according to the strategy shown in **Figure 2** (right). This "all-in-one" approach is expected to increase the processing rate and to reduce the production costs by decreasing the number of dipping steps while maintaining a high AB activity and durability.

The formation of nanogels Pox(mDOPA)/PAH that are not silver loaded was first studied by the slow addition of a solution of PAH (1 g L^{-1}) to an aqueous solution of Pox(mDOPA) at room temperature (see ESI, Supporting Information Figure S4, (**a**)). Weight ratios and addition modes of the two partners were controlled to form stable dispersions of nanogels (Pox(mDOPA)/PAH). For that purpose, the slow addition of PAH (1 g L^{-1}) to an aqueous solution of Pox(mDOPA) (1 g L^{-1}) resulted in the spontaneous formation of a stable and clear light brown solution of cross-linked nanogels at room temperature. The presence of the nanogels was confirmed by TEM that showed nanogels with a diameter ranging from 20 to 30 nm (**Figure 3**A). It is important to note that the nanogels solution had to be lyophilized on the TEM grid prior to analysis. If the solution was simply dropped onto the grid and slowly dried at room temperature under atmospheric conditions, nanogels strongly aggregated (see ESI, Supporting Information Figure S5A). Analysis by dynamic light scattering (DLS) without filtration showed nanogels agglomeration with an average hydrodynamic diameter equal to 120 ± 30 nm with a rather high polydispersity (PDI = 0.2) (see ESI, Supporting Information Figure S6). The nanogels solutions were stable for at least one month when stored at room temperature and at pH around 10 without stirring. Indeed, the solution remained clear without any precipitation and the hydrodynamic diameter distribution obtained by DLS remained almost unchanged after one month of storage (see ESI, Supporting Information Figure S6).

The cross-linking reaction through the amine/quinone reaction has been proven by solid state ^{13}C NMR analysis of the lyophilized product with typical signals around 160 ppm assigned to the newly formed imine bonds (**Figure 4**b), coming from the Schiff base formation. The Michael addition is also expected to occur but cannot be evidenced on the basis of the NMR experiment. Moreover, the freeze-dried solution cannot

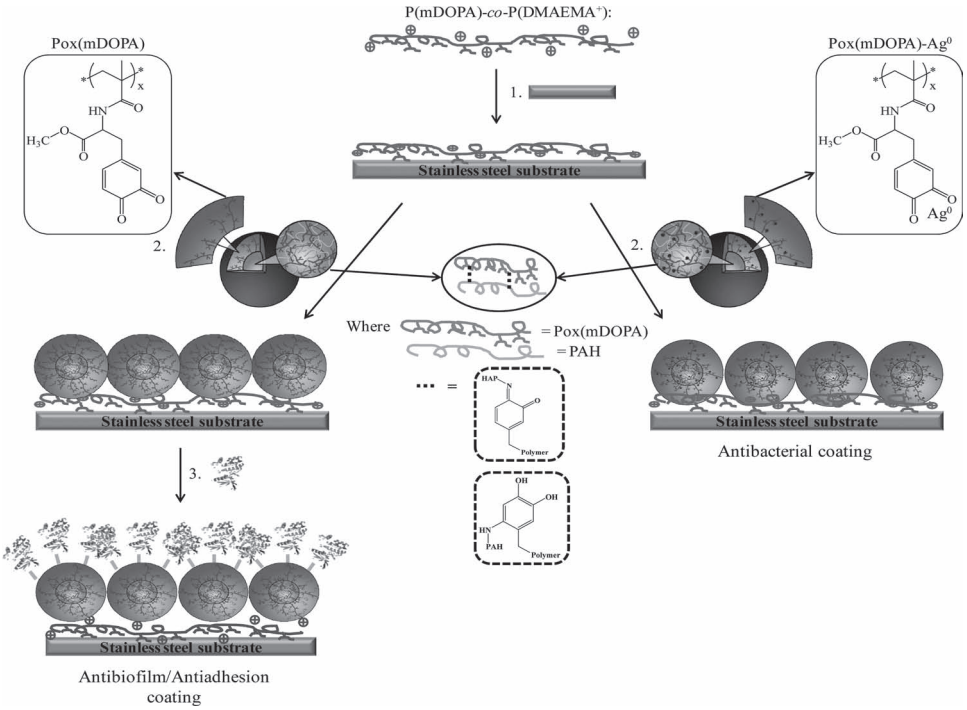

Figure 2. Formation of AB films from silver loaded nanogels (Pox(mDOPA)-Ag^0/PAH) (right) and antibiofilm/antiadhesion coatings by immobilization of DspB and PEG-SH onto (Pox(mDOPA)/PAH) nanogels (left).

be re-dispersed in any solvent indicating that the nanogels were cross-linked.

The deposition of the nanogels onto SS was then followed by QCM-D. First, an aqueous solution of the biomimetic glue, P(mDOPA)-*co*-P($DMAEMA^+$) (2 g L^{-1}), was flowed through the cell at room temperature, leading to the first anchoring layer (see ESI, Supporting Information Figure S7). After removing the excess unbounded polymer by rinsing with water, the deposition of the nanogels solution was observed by the important decrease of the frequency vibration.[20] Importantly, this layer of nanogels was stable since it cannot be removed after rinsing with water. Flowing the cell with PAH then led to the deposition of this polymer that served as anchoring layer between two nanogels layers by the reaction of primary amines of PAH with residual quinone groups present in the nanogels. Rinsing steps between each layer were applied to remove excess polymer before the deposition of the next layer. The ellipsometry measurements of a monolayer of nanogels Pox(mDOPA)/PAH on

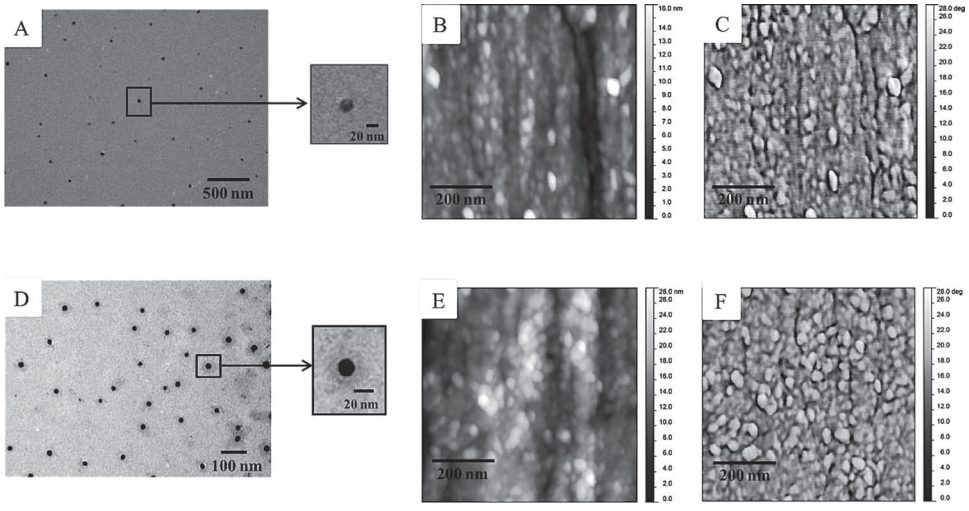

Figure 3. TEM images of nanogels Pox(mDOPA)/PAH solution after lyophilisation (A) and AFM investigations of a monolayer of nanogels Pox(mDOPA)/PAH on SS pre-coated by the biomimetic glue (B: topographic image, C: phase signal). TEM image of silver loaded nanogels Pox(mDOPA)-Ag^0/PAH solution after lyophilization (D) and AFM investigations of a monolayer of silver loaded nanogels Pox(mDOPA)-Ag^0/PAH on stainless steel pre-coated by the biomimetic glue (E: topographic image, F: phase signal). AFM image dimensions: 600 nm × 600 nm.

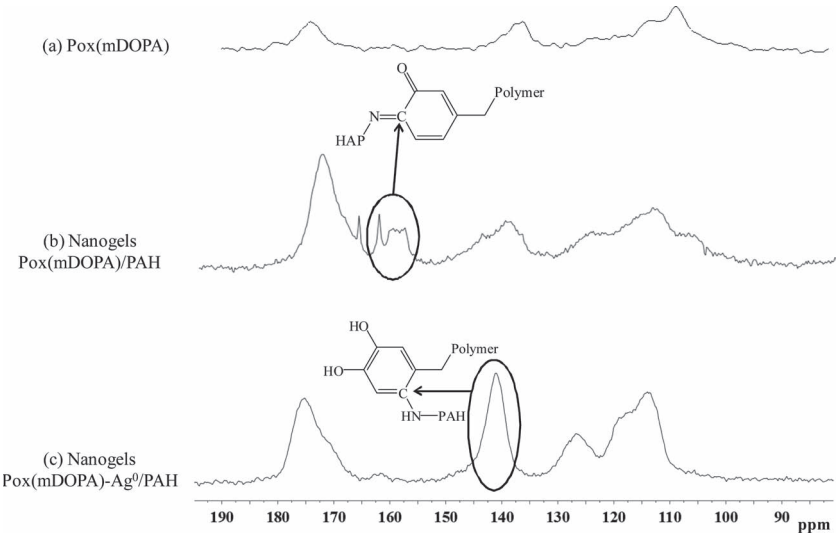

Figure 4. ^{13}C NMR spectra in the solid state of a) Pox(mDOPA), b) nanogels Pox(mDOPA)/PAH, and c) silver loaded nanogels Pox(mDOPA)-Ag^0/PAH.

stainless steel pre-coated by the biomimetic glue predicted a thickness of 10–12 nm.

Antibacterial nanogels (Pox(mDOPA)-Ag^0/PAH) were then prepared in a similar way by the addition of a PAH solution (1 g L^{-1}) to an aqueous solution of silver loaded Pox(mDOPA) (see ESI, Supporting Information Figure S4, (**b**)), resulting in the appearance of a milky-yellow-brown suspension that is stable for about 5 days. TEM evidenced the formation of spherical nanogels whose sizes range from 20 to 30 nm (Figure 3D). The suspension was lyophilized in order to fix the system and avoid particle agglomeration that is observed when the solution is dried under atmospheric conditions at room temperature on the TEM grid (see ESI, Supporting Information Figure S5B). DLS measurement without filtration (see ESI, Supporting Information Figure S8) evidenced the presence of some nanogels agglomeration with an average hydrodynamic diameter of 200 nm (± 50 nm) with a rather high polydispersity (PDI = 0.2). Moreover, the lyophilized nanogels cannot be re-dispersed in water suggesting that the nanogels are cross-linked. Solid-state ^{13}C NMR of these lyophilized nanogels was then carried out. In contrast to cross-linked nanogels that are not silver loaded, the silver loaded ones presented only a slight peak around 160 ppm assigned to the imine bond. On the other hand, the intensity of the signal at 140 ppm (already observed on Pox(mDOPA) and assigned to C=C bond in *o*-position of the quinone groups) strongly increased in the silver loaded cross-linked system. This intensity increase was the result of =C-NH- formed by Michael addition of the primary amine of PAH to the quinone groups of Pox(mDOPA) (Figure 4c). This significant difference between silver loaded and unloaded nanogels is certainly the result of the complexation of the quinone groups by the silver nanoparticles that avoids the Schiff base formation to the benefit of the Michael addition.

Through AFM investigation, the formation of a monolayer of nanogels Pox(mDOPA)/PAH on stainless steel pre-coated by the biomimetic glue was observed (Figure 3B,C). In the case of the monolayer assembled by silver loaded nanogels Pox(mDOPA)-Ag^0/PAH, the morphology of the outer layer was analogous (Figure 3E). A signature of the presence of Ag particles was not evident in phase contrast (Figure 3F) and the metal nanoparticles were difficult to be located without any doubt in the topographic images due to the similar dimension of the grains of the stainless steel surface. The roughness has been evaluated for the different surfaces on several areas of 600 × 600 nm^2 giving the following values: 2.3 ± 0.5 nm in the case of clean SS, 2.7 ± 0.2 nm in the case of nanogels Pox(mDOPA)/PAH and 6.1 ± 0.9 nm in the case of silver loaded nanogels Pox(mDOPA)-Ag^0/PAH. The comparable roughness between clean SS and nanogels Pox(mDOPA)/PAH reflected the capability of the nanogels to follow the morphology of the substrate. The presence of the Ag^0 particles inside the monolayer can be therefore inferred by the increased roughness measured in the case of nanogels Pox(mDOPA)-Ag^0/PAH on respect of nanogels Pox(mDOPA)/PAH and of uncoated stainless steel surfaces.

AB coating was then formed by dipping the substrate, precoated by a layer of the biomimetic glue, into the nanogels Pox(mDOPA)-Ag^0/PAH solution for 2 min at room temperature. After rinsing with water to remove unbounded nanogels, the AB test was realized against *E. coli* by the same method used for the multilayer (P(mDOPA)-*co*-P($DMAEMA^+$)/[(Pox(mDOPA)-Ag^0/PAH)$_5$]). Bare SS and the coating without silver nanoparticles ((P(mDOPA)-*co*-P($DMAEMA^+$)/[(Pox(mDOPA)/PAH)]) showed no AB activity in these conditions (**Table 2**, entries **1** and **2**). The silver loaded coating killed all bacteria after only 1 h of incubation (Table 2, entry **3**). Its activity was maintained at the same level even when dipping the coated substrate into a NaOH aqueous solution (0.1´M) for one night (Table 2, entry **7**). Dipping it into water at room temperature or at 50 °C did not increase its AB activity significantly since all bacteria were killed after 2 h of incubation (Table 2, entries **4** and **5** respectively). When the coating was cleaned with a wet sponge (25 forth and back movements) or dipped into diluted hhc, it remained active but required a longer period of time to kill all bacteria (Table 2, entries **6** and **8** respectively). For the sake of comparison, when poly(ethylenimine) (PEI) substituted our biomimetic glue (P(mDOPA)-*co*-P($DMAEMA^+$)) as the first layer, the AB activity was immediately lost after overnight immersions in the same conditions (diluted hhc, basic water, etc.) (data not shown). This control experiment demonstrated that our copolymer bearing DOPA moieties is once again necessary for anchoring the coating on the SS surface and for preserving the AB activity.

In contrast to the previous section with the multilayer film, the AB activity of the substrate coated with the silver loaded nanogels was not affected when immersed in hot water (50 °C) overnight prior to AB testing. Indeed, the cross-linking occurred mainly during the nanogels formation before their deposition on the substrate.

Finally, antibacterial activity of these silver-loaded nanogels was demonstrated against Gram positive bacteria, *Staphylococcus*

Table 2. Antibacterial activity of SS substrates covered or not by DOPA-based nanogels against *E. coli* (T_0 = 3 10^5 cell mL^{-1}; T_0 = initial number of bacteria per mL used for the test).

Entry	Sample	1 h of contact		2 h of contact		19 h of contact	
		Cell mL^{-1} [a]	Reduction rate [%]	Cell mL^{-1} [a]	Reduction rate [%]	Cell mL^{-1} [a]	Reduction rate [%]
1	Bare SS	1.1×10^6	–	3×10^6	–	1.3×10^7	–
2	Nanogels[b]	5.2×10^5	–	9.9×10^5	–	1.8×10^7	–
3	Silver loaded-nanogels[c] Control[c]	0	100	0	100	0	100
4	Immersed in cold water	5×10^4	83	0	100	0	100
5	Immersed in hot water	3×10^4	90	0	100	0	100
6	Immersed in diluted hhc	2×10^5	33	1.5×10^5	50	0	100
7	Immersed in basic medium	0	100	0	100	0	100
8	Mechanical test	1.9×10^5	37	8×10^4	73	0	100

[a] Survival number of bacteria mL^{-1}; [b] P(mDOPA)-*co*-P(DMAEMA$^+$)/nanogels (Pox(mDOPA)-PAH); [c] P(mDOPA)-*co*-P(DMAEMA$^+$)/nanogels (Pox(mDOPA)-Ag^0/PAH).

epidermidis (*S. epidermidis*). Although a longer period of time was needed to kill all bacteria, films were also active against this strain even after applying the different durability treatments discussed above (see ESI, Supporting Information Table S1).

It is important to mention here that stainless steel covered by nanogels that are not silver loaded have no antibacterial activity against both bacteria strains, *E. coli* (Table 2, entry 2) and *S. epidermidis* (Supporting Information Table S1, entry 2). This clearly demonstrates that the uppermost layer of the coating is not antibacterial and that silver particles are necessary for the AB activity.

2.3. Pox(mDOPA)/PAH Multilayer Film for the Grafting of Antibiofilm/Antiadhesion (Bio)Molecules

Another method to provide hygienic surfaces is to avoid bacteria to adhere to the surface and to form a resistant biofilm that is a source of infection.[21] Examples of antiadhesion/antibiofilm coatings comprise polymers (poly(ethylene glycol) (PEG)[22] or poly(sulfobetaine methacrylate))[23] as well as enzymes.[24] In this study, the antiadhesion properties of PEG and the antibiofilm activity of an enzyme, DispersinB (DspB), will be considered to illustrate the versatility and efficiency of our coating processes.

Poly(ethylene glycol) (PEG) is one of the most commonly used synthetic polymer to impart protein resistance to a surface.[25] Several strategies to modify substrates with that kind of polymers can be found in the literature such as electrografting,[26] self-assembled monolayers (SAMs),[27] copolymers adsorption,[28] polymers grafting[29] or initiated from the surface[30] to cite only a few.

DispersinB (DspB) is an enzyme active against *N*-acetylglucosamine-containing extracellular polysaccharides that are a part of biofilms. It consequently degrades the polysaccharides that the bioorganisms use to anchor and colonize the substrates.[31] Furthermore, this water-soluble enzyme is highly active against both Gram negative[32] and positive[33] bacteria such as *E. coli* and *S. epidermidis*, respectively. This enzyme has already been physically trapped into coatings and was released in the media when biofilm appeared on the surface.[33,34] There are also few publications reporting on the immobilization of enzymes on materials to confer antibacterial properties to surfaces.[35]

In order to impart long-term durability to the coating and prevent biofilm formation when SS is ageing, we are considering the covalent anchoring of PEG and DspB onto SS surfaces. The DOPA quinone containing coatings developed above are selected in our study for their environmental friendly experimental conditions (only aqueous solutions are used at room temperature), their simplicity and ease to scale-up.

The (bio)molecule grafting was carried out by exploiting the reactivity of quinone groups of Pox(mDOPA) (**2**, Figure 1) towards thiols.[11c,36] For that purpose, thiol end-functionalized PEG (PEG-SH) and DspB that contains two external cysteines (and thus thiol groups) in its sequence were considered for the conjugation. This thiol-based strategy allows specific enzyme grafting under mild conditions and without pH constrain in contrast to the amino-based strategy that requires pH ≥ 10.[37]

When enzymes are considered, such as DspB, there is often an optimal pH range at which they present the highest activity. The optimum pH for DspB was thus first evaluated in solution (see ESI, Supporting Information Figure S9) upon hydrolysis of a chromogenic substrate 4-nitrophenyl-β-D-*N*-acetylglucosaminide by DspB. It results in the formation of a yellow product, *p*-nitrophenol, which absorbs at 405 nm. Following the increase of this absorbance value, optimum pH was 5.9 (see ESI, Supporting Information Figure S9). Importantly, at this pH value, amino groups of DspB are positively charged and are thus not reactive towards the quinone groups of the coating. A selective grafting of DspB through one of its thiol groups (that are not essential for its enzymatic activity) is thus expected to occur through Michael type addition. Denaturation of the enzyme by multiple grafting sites to the surface should therefore be avoided when working at this pH value.

DspB was then grafted at room temperature and pH 5.9 on a 5-bilayers cross-linked film (P(mDOPA)-*co*-P(DMAEMA$^+$)/[(Pox(mDOPA)/PAH)$_5$]) composed of a first glue layer (P(mDOPA)-*co*-P(DMAEMA$^+$)) and 5 bilayers of cross-linked Pox(mDOPA) and PAH (strategy described in the above section). In order to render the surface reactive towards the

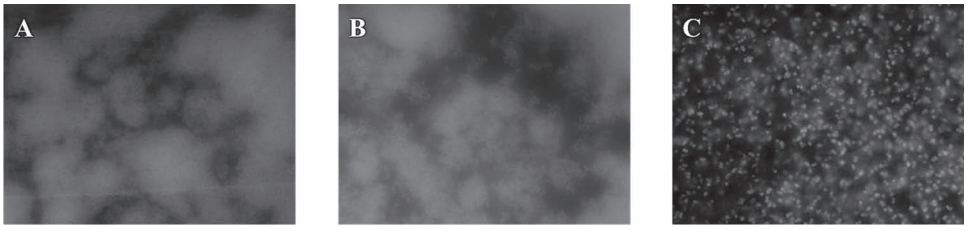

Figure 5. Fluorescence images of *Staphylococcus epidermidis* biofilm forming on bare stainless steel (A), P(mDOPA)-*co*-P(DMAEMA$^+$)/[(Pox(mDOPA)/PAH)$_5$] (B), and P(mDOPA)-*co*-P(DMAEMA$^+$)/[(Pox(mDOPA)/PAH)$_5$]-DspB (C); magnification 1000×.

enzyme grafting, the last layer is Pox(mDOPA) (see ESI, Supporting Information Figure S10).

X-ray Photoelectron Spectroscopy (XPS) confirmed the presence of DspB on these multilayers by the detection of its sulfur atoms (see ESI, Supporting Information Figure S11). Furthermore, the content of active DspB immobilized on such coatings has been evaluated around 1.94 ± 0.2 μg cm^{-2} thanks to a calibration curve (see ESI, Supporting Information Figure S12).

Its antibiofilm activity was then first qualitatively evaluated against *S. epidermidis* after labeling with a fluorescent dye. Pictures taken under epifluorescence microscope after 24 h of biofilm formation are summarized in **Figure 5**. Bare SS and P(mDOPA)-*co*-P(DMAEMA$^+$)/[(Pox(mDOPA)/PAH)$_5$]-coated SS are covered with a thick biofilm as traduced by the presence of large clusters of glued and static bacteria in a wadded matrix (Figure 5A,B, respectively). In comparison, Figure 5C shows the DspB-coated SS. Large population of scattered bacteria, in constant motion (when observed at the microscope), and few moving wadded clusters were observed as an indication of less/no biofilm formation.

Impact of grafted DspB on *S. epidermidis* biofilm was then quantified. The number of viable *S. epidermidis* adherent bacteria was decreased by 97% (standard deviation: 3%) on DspB-coated surfaces (**Table 3**, entry 2) compared to their uncoated counterparts. The statistics were made on three samples.

In parallel, PEG-SH was also anchored to these DOPA-containing 5-bilayers coatings following the same grafting strategy as for DspB. Antiadhesion activity of these coatings has also been assessed quantitatively against *S. epidermidis*. Immobilized-PEG-SH coatings were also active against *S. epidermidis* as traduced by 93% decrease of the adherent bacteria compared with the uncoated counterparts (standard deviation: 12%) (Table 3, entry 3). Importantly, all these assessments are done on coatings that are rinsed for 24 h with water to remove non-grafted antibiofilm/antiadhesion (bio)molecules. It clearly highlights that the activity is therefore preserved even after long immersion periods, in agreement with the covalent grafting of the active species to the coating. It is important to note that the same multilayer coating without DspB or PEG-SH (P(mDOPA)-*co*-P(DMAEMA$^+$)/(Pox(mDOPA)/PAH)$_5$; Table 3, entry 1) had no antibiofilm activity and did not reduce the amount of adherent bacteria. It clearly demonstrates that the uppermost layer of the multilayer coating (Pox(mDOPA) and eventually residual uncovered PAH) has no antibiofilm activity.

Although this strategy based on 5-bilayers coating is highly active to reduce the population of bacteria on the surface, it presents the same major drawback as for the silver loaded multilayer film: the long processing time. The LbL process for the film building takes about 45 min to get SS ready for grafting with DspB or PEG-SH.

2.4. Nanogels Pox(mDOPA)/PAH for the Grafting of Antibiofilm/Antiadhesion (Bio)Molecules

In order to shorten the processing time, these active molecules coupling strategies were transposed onto the water-based cross-linked nanogels film presented in the previous section (Figure 2, (left)). The surface coated by a layer of the glue, P(mDOPA)-*co*-P(DMAEMA$^+$), and a layer of the nanogels Pox(mDOPA)/PAH, was then incubated with the aqueous solutions of DspB or PEG-SH following the same grafting conditions described above. The film building with DspB was confirmed by QCM-D on stainless steel sensors as shown on **Figure 6**. All the partners

Table 3. Antibiofilm/antiadhesion activity against *S. epidermidis* biofilm forming of modified-SS surfaces compared to uncoated ones. n is the number of samples on which statistics are based.

Entry			% Reduction of adherent population
1		P(mDOPA)-*co*-P(DMAEMA$^+$)/[(Pox(mDOPA)/PAH)$_5$]	0 (n = 3)
2	Multilayer film composition	P(mDOPA)-*co*-P(DMAEMA$^+$)/[(Pox(mDOPA)/PAH)$_5$]-DspB	97 ± 3 (n = 3)
3		P(mDOPA)-*co*-P(DMAEMA$^+$)/[(Pox(mDOPA)/PAH)$_5$]-PEGSH	93 ± 12 (n = 6)
4		P(mDOPA)-*co*-P(DMAEMA$^+$)/[nanogel(Pox(mDOPA)/PAH)]	0 (n = 3)
5		P(mDOPA)-*co*-P(DMAEMA$^+$)/[nanogel(Pox(mDOPA)/PAH)]-DspB	86 ± 9 (n = 6)
6	Bilayer nanogels composition	P(mDOPA)-*co*-P(DMAEMA$^+$)/[nanogel(Pox(mDOPA)/PAH)]-PEGSH	93 ± 4 (n = 6)
7		P(mDOPA)-*co*-P(DMAEMA$^+$)/PSS-DspB	54 ± 35 (n = 6)
8		P(mDOPA)-*co*-P(DMAEMA$^+$)/PSS-PEGSH	70 ± 15 (n = 6)

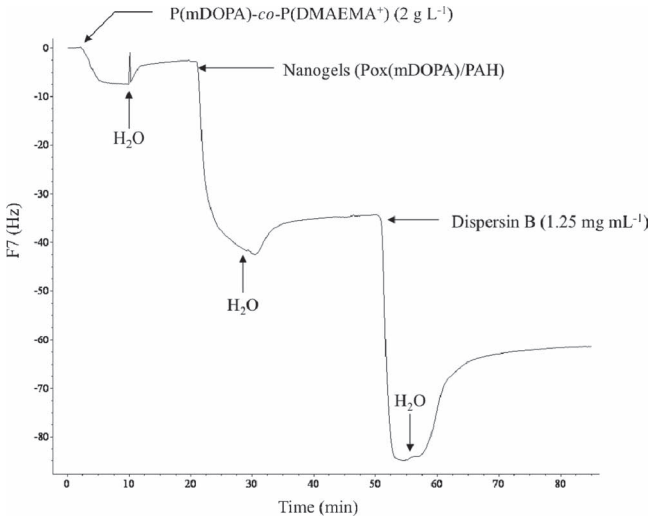

Figure 6. Frequency change upon deposition of P(mDOPA)-*co*-P(DMAEMA$^+$), [nanogel(Pox(mDOPA)/PAH)] and DspB measured by QCM-D as a function of time at 25 °C, where the overtone number is 7.

were well inserted into the film and remained on the substrate after the rinsing steps with deionized water.

The presence of DspB (1.64 ± 0.41 μg cm^{-2} according to the calibration curve) was then confirmed by quantifying the antibiofilm activity of the coated substrates (Table 3, entry 5). Antibiofilm activity of DspB-coatings was maintained with 86% of reduction of adherent population of *S. epidermidis* (standard deviation: 9%) even when the surface was immersed in PBS buffer for 24 h before testing. The same behavior was observed when PEG-SH was immobilized onto the nanogels coatings with 93% of reduction of the adherent population (standard deviation: 4%) (Table 3, entry 6).

Finally, in order to demonstrate the importance of the film covalent cross-linking and covalent grafting of the active molecule (DspB and PEG-SH) on the film activity, a LbL film formed by electrostatic interactions instead of covalent ones was built and post-modified by DspB or PEG-SH. This bilayer electrostatic film was formed by alternating the deposition of a negatively charged polyelectrolyte, poly(styrene sulfonate) (PSS at 2 g L^{-1}) on a cationic one, P(mDOPA)-*co*-P(DMAEMA$^+$). Lower antibiofilm and antiadhesion activities were observed on those films and higher standard deviations were noted, showing significant variability when electrostatic adsorptions are considered (Table 3, entries 7 and 8). This clearly showed the benefit of the permanent immobilization of the active molecules on the surfaces.

3. Conclusions

In this work, we have developed an environmental friendly and simple procedure for coating substrates (stainless steel in this case) with antibacterial, antibiofilm and antiadhesion molecules. The long-term durability of the functionality has been guaranteed by the combination of a bio-inspired glue, the film cross-linking and by covalently anchoring the active (bio)molecules at the surface of the coatings in mild reaction conditions. The chemical reaction responsible for the strong adhesion of the active coating (multilayers and nanogels) to the bio-inspired glue is however still unknown and under investigation. On the other hand, the chemistry involved in the cross-linking deals with the highly reactive quinone/amine and quinone/thiol pairs. Two types of reactive cross-linked films were considered in this study. The first one involves the alternative deposition of aqueous solutions of a polymer bearing quinone groups (Pox(mDOPA)) with a polymer bearing primary amines (PAH). Antibacterial coatings can be built by doping them with silver nanoparticles in situ formed while antibiofilm and antiadhesion properties have been imparted by covalent grafting of an enzyme (DispersinB) and poly(ethylene glycol), respectively, to the last layer of the film. This covalent bonding has been ensured by the reaction of thiol group of the active (bio)molecule (DspB or PEG-SH) with the quinone groups of the outer Pox(mDOPA) film layer. The second strategy investigated in this study is even more interesting since it is very simple, versatile, easily scalable and allows fast surface modifications in mild conditions. Indeed, we have for the first time synthesized novel reactive nanogels using a one step procedure by mixing aqueous solutions of Pox(mDOPA) with PAH in appropriate proportions. Their deposition on a substrate precoated by a biomimetic glue allows further surface derivatizations. Proof of concept has been notably demonstrated by the grafting of enzyme (DspB) or PEG-SH that promote long-term activity to the substrate. This ready-to-use solution of nanogels is very simple to prepare and the coating strategy developed in this work is very suited for imparting various activity to surfaces from aqueous solutions by the grafting of various molecules, including biomolecules such as enzymes without denaturation. These nanogels constitute therefore interesting platforms towards further surface modifications.

4. Experimental Section

Materials: Poly(allylamine) hydrochloride (PAH; M_w = 15 000 g mol^{-1}), O-[2-(3-Mercaptopropionylamino)ethyl]-O′-methylpolyethylene glycol (PEG-SH, M_w = 5000 g mol^{-1}), poly(styrene sulfonate) (PSS, M_w = 70 000 g mol^{-1}), silver nitrate ($AgNO_3$) and poly(ethylenimine) (PEI; M_w = 25 000 g mol^{-1}) were purchased from Sigma-Aldrich and used without further purification. Synthesis of P(mDOPA)-co-P(DMAEMA$^+$) (15 mol% DOPA determined by UV-vis spectroscopy) and P(mDOPA) were described in our previous publications.[12,15] Fatty alcohol ethoxylates based household cleaner (hhc) was commercially available by Bref. Nutrient media for antibacterial/antibiofilm/antiadhesion assessments: BactoTryptone, BactoYeast Extract and Bacto Casamino Acids were obtained from Becton Dickinson (USA). Agar-agar was purchased from Merck (USA). Luria-Bertani medium (LB) was prepared with BactoTryptone(10 g), Bacto Yeast Extract(5 g), and NaCl (10 g) in DI water (1 L). LB agar medium was obtained by adding agar-agar (15 g) in LB (1 L). M63 medium containing 100 mM KH_2PO_4, 15 mM $(NH_4)_2SO_4$, 1.6 mM, $MgSO_4$, 4 μM $FeSO_4$, pH 5.9 was supplemented with 0.5% casamino acids and 0.2% glucose.

Expression and Purification of Recombinant DspB Protein: i) Plasmid pET28aDspB was bought from Geneart (Life Technologies, UK) and used for the overexpression of the DspB enzyme. Four 2-liter Erlenmeyer flasks containing Luria-Bertani broth (500 mL) supplemented with kanamycin (30 μg mL^{-1}) were inoculated with an overnight culture of E. coli strain BL21(DE3)Star transformed with pET28aDspB (5 mL). The

flasks were incubated at 37 °C with agitation (200 rpm) until the optical density of the culture at 600 nm reached 0.6 (ca. 3 h). IPTG was added to a final concentration of 0.5 mM, and the flasks were incubated for an additional 4 h with agitation. The cells were harvested by centrifugation for 15 min at 6000 × g, and the cell pellets were stored at −20 °C. ii) Protein purification. The cell pellets were thawed at room temperature and re-suspended in washing buffer (20 mM Na_2HPO_4-NaH_2PO_4 (PO_4) pH 7.2, 1% NaCl). The cell suspension was then centrifuged 20 min at 4000 rpm. Harvest cells were re-suspended in lyses buffer (100 mL; 20 mM PO_4 pH 7.2, 500 mM NaCl, $MgSO_4$ 10 mM, antiprotease coktail) and disrupted with the emulsiflex. DNA was digested with Benzonase (5 µL). The cell debris was pelleted by centrifugation at 15 000 × g for 20 min at 4 °C.

The supernatant was loaded onto a 5-mL (bed volume) HiTrap Chelating column (Pharmacia) according to the instructions supplied by the manufacturer. The column was washed with wash buffer (50 mL; 20 mM PO_4 pH 7.2, 500 mM NaCl). The protein was eluted with a gradient of 20 mM PO_4 pH 3.5, 500 mM NaCl buffer. The purification process was repeated three times in order to load the whole sample. Fractions of the elute were collected and assayed for the presence of the protein by sodium dodecyl sulfate (SDS)-polyacrylamide gel electrophoresis and Coomassie blue staining. Fractions containing the protein were pooled and dialyzed overnight against 10 mM PO_4 pH 5.9, 100 mM NaCl by using a 10 000-kDa-cutoff dialysis membrane. Proteins were quantified thanks to the BCA kit (Pierce). Mass spectra after trypsin digestion was recorded on the SDS gel band containing the dispersinB protein.

Enzyme Assays: The chromogenic substrate 4-nitrophenyl-N-acetyl-β-D-galactosaminide (Sigma Aldrich) was used to characterize DispersinB activity. Enzyme reactions were carried out in 1-mL mixtures containing 50 mM sodium phosphate buffer (at pH 5.9, 6.5 or 7.6), 100 mM NaCl, 5 mM substrate, and purified protein (3.7 µg mL^{-1}) in 1.5-mL polypropylene tubes placed in a 37 °C water bath. The reactions were terminated at various times (20 min max) by adding 10 N NaOH (5 µL). The increase in absorption resulting from the release of *p*-nitrophenolate in each tube was measured with a Viktor X3 Perkin-Elmer spectrophotometer set to 405 nm.

A calibration curve of DispersinB activity in solution has also been conducted following the same procedure as described above (see ESI, Supporting InformationFigure S12). Note that extreme values at high absorbance were obtained from diluted solutions. Measurements of the enzyme activity on the substrates were made possible by incubating 160 µL of a solution containing 50 mM sodium phosphate buffer (at pH 5.9), 100 mM NaCl and 5 mM substrate on the modified SS-surfaces during 30 min at 37 °C. 120 µL were then collected from the samples, transferred to a 96-well plate and absorbance was measured at 405 nm using a spectrophotometer Perkin Elmer (2030). As a control, 4-nitrophenyl-N-acetyl-β-D-galactosaminide solution has an absorbance around 0.08. Statistics were made on four replicates.

Oxidation of P(mDOPA) in Basic Medium: Oxidation is carried out according to a procedure reported elsewhere.[15] P(mDOPA) (20 mg) are dissolved in distilled water (10 mL) and a NaOH solution (0.1 M) is slowly added in order to raise the pH above 10. This oxidation step lasts at least one night under air and is followed by UV Vis spectroscopy.

Formation of the Pox(mDOPA)-Ag^0 Hybrid: P(mDOPA) (20 mg) are dissolved in distilled water (9 mL) and $AgNO_3$ (1 mL; $7.1.10^{-3}$ M) (molar ratio DOPA/Ag: 1/1) is slowly added in the dark under vigorous stirring at room temperature. The final suspension was stirred for 20 h before coating.

Silver nanoparticles with a diameter ranging between 3 and 7 nm are observed by transmission electron microscopy (TEM) (see ESI, Supporting Information Figure S2).

Preparation of Pox(mDOPA)/PAH Cross-Linked Nanogels: P(mDOPA) (10 mg) are dissolved in distilled water (10 mL) and NaOH (0.1 M) is slowly added in order to raise the pH above 10 in order to promote the oxidation of catechol groups of P(mDOPA). After one night at room temperature, an aqueous solution of PAH (3 mL; 1 g L^{-1}) at pH 10 are slowly added to the solution of Pox(mDOPA) under vigorous stirring. The solution is lead to react for one h at room temperature under vigorous stirring. Nanogels with a diameter ranging from 20 to 30 nm are observed by TEM (Figure 3A). The nanogels cross-linking formation was observed by solid state ^{13}C NMR of the lyophilized product by the appearance of typical signals around 160 ppm (Figure 4b) assigned to the newly formed imine bonds, coming from the Schiff base formation.

Preparation of Pox(mDOPA)-Ag^0/PAH Hybrid Nanogels: P(mDOPA) (10 mg) are dissolved in distilled water (9 mL) and an aqueous solution of $AgNO_3$ (1 mL; $3.5.10^{-2}$ M) (molar ratio DOPA/Ag: 1/1) is slowly added in the dark under vigorous stirring at room temperature. The suspension is stirred for 20 h. Then, a PAH solution (3 mL; 1 g L^{-1} in water) at pH 10 are slowly added under vigorous stirring. The solution is lead to react for one h at room temperature under vigorous stirring. Nanogels with a diameter ranging from 20 to 30 nm are observed by TEM (Figure 3D). The nanogels cross-linking formation was observed by solid state ^{13}C NMR (Figure 4c) that evidences the formation of Michael type addition product at around 140 ppm.

Silver-Loaded Multilayer Film Assembly: LbL deposition is conducted at room temperature. Stainless steel 304 2B surfaces (SS) were supplied by CRM Group AC&CS (Belgium), cleaned with acetone and ethanol (scrubbing with an optical tissue) and dried under argon. Small surfaces (2 cm × 2 cm) were immediately dipped into the first copolymer solution: P(mDOPA)-*co*-P($DMAEMA^+$) for 2 min. The following cycle was then used for five bilayers: 1) Pox(mDOPA)-Ag^0 for 2 min, 2) rinse twice in water for 1 min each, 3) PAH (M_w = 15000 g mol^{-1}, Sigma-Aldrich) for 2 min, 4) rinse twice in water for 1 min each. The uppermost layer is comprised of Pox(mDOPA)-Ag^0. One control experiment was also conducted following the same cycles but using PEI at a concentration of 8 g L^{-1} NaCl 0.15 M as the first layer instead of P(mDOPA)-*co*-P($DMAEMA^+$). Concentrations of all polymers were 2 g L^{-1} in distilled water (pH ≈ 11, adjusted by NaOH 0.1 M).

Multilayer Film Assembly and Grafting of Active Molecules Bearing Thiol(s): The procedure is identical as the one described above except that Pox(mDOPA) is used instead of Pox(mDOPA)-Ag^0 to build a five bilayers film on SS: P(mDOPA)-*co*-P($DMAEMA^+$)/[(Pox(mDOPA)/PAH)$_5$], the last layer being Pox(mDOPA). DspB was then grafted by incubating the enzyme solution (100 µL) at 1.25 mg mL^{-1} in PBS buffer (50 mM) at pH 5.9 and NaCl 100 mM for one h at room temperature. The same strategy has been applied to PEG-SH solution at 10 mg mL^{-1} in milliQ water. Active molecules-grafted substrates were then rinsed 6 × 1 min at room temperature and 20 h at 6 °C in 2 mL-aliquots of PBS buffer at pH 5.9 or milliQ water for DspB and PEG-SH respectively. They were finally kept at 6 °C before any antibiofilm or antiadhesion activity assessment.

Silver-Loaded Bilayer Nanogels Assembly: Nanogels LbL deposition is conducted at room temperature. Stainless steel 304 2B surfaces (SS) are supplied by CRM Group & AC&CS (Belgium), cleaned with acetone and ethanol (scrubbing with an optical tissue) and dried under argon. Small SS surfaces (2 cm × 2 cm) are immediately dipped into the glue solution (P(mDOPA)-*co*-P($DMAEMA^+$); 2 g L^{-1}) for 2 min. After rinsing twice with water for 1 min, the modified substrates are dipped into a solution of nanogels Pox(mDOPA)-Ag^0/PAH for 2 min and rinsed twice with water for 1 min. A control experiment is also conducted following the same cycles but using PEI at a concentration of 8 g L^{-1} in NaCl 0.15 M as the first layer instead of the glue solution (P(mDOPA)-*co*-P($DMAEMA^+$)).

Bilayer Nanogels Assembly and Grafting of Active Molecules Bearing Thiol(s): The procedure is identical as the one described above except that nanogels Pox(mDOPA)/PAH are used instead of the Pox(mDOPA)-Ag^0/PAH ones. The strategy for grafting active molecules was the same as the one described here above for multilayer films. An electrostatic control experiment has also been conducted following the same procedure but replacing the nanogels layer by a poly(styrene sulfonate) one (PSS, 2 g L^{-1}).

Characterization Methods: DOPA contents are determined by UV-vis spectroscopy with a Hitachi spectrophotometer (U-3300) at room temperature starting from a dopamine calibration curve.

Film growths (multilayers and nanogels ones) were followed in real time using quartz crystal microbalance coupled with dissipation

technique (QCM-D). A Q-Sense E4 is used in this study. The stainless steel-coated AT-cut resonator (fundamental frequency: 5 MHz) is used as received. First, distilled water is introduced in the cell and the flow is maintained until a stable baseline is obtained. LbL deposition is then initiated by switching the liquid exposed to the crystal from distilled water to the glue solution (P(mDOPA)-*co*-P(DMAEMA$^+$); 2 g L^{-1} with 0.15 M NaCl) at a flow rate of 250 µL min^{-1}, temperature of 25.09 ± 0.02 °C. After 10 min, the substrate is rinsed by distilled water to remove the excess of unbounded glue. Then, the alternative deposition of nanogels Pox(mDOPA)/PAH (1 g L^{-1}) and PAH (1 g L^{-1}) solutions is carried out (about 10 min for each step) with rinsing steps with distilled water between each layer. Active molecule solution (DspB or PEG-SH) was finally introduced in the system and further rinsed when a stable signal is obtained.

Energy-dispersive X-ray spectra of the silver loaded coatings are recorded using a field emission gun scanning electron microscope (FEG-SEM) MEB ULTRA55 operating at 3 kV coupled with a energy-dispersive X-ray spectrometer.

Ellipsometry measurements are done using a SOPRA GES 5 working in the UV-Visible range from 300 up to 900 nm. The angle of incidence is 75°.

The XPS analyses were performed on a SSX 100/206 photoelectron spectrometer from Surface Science Instruments (USA) equipped with a monochromatized micro focused Al X-ray source (powered at 20 mA and 10 kV). The pressure in the analysis chamber was around 10^{-6} Pa. The angle between the surface normal and the axis of the analyser lens was 55°. The analysed area was approximately 1.4 mm^2, the analysed depth comprised between 1–10 nm and the pass energy was set at 150 eV. In these conditions, the full width at half maximum (FWHM) of the Au $4f_{7/2}$ peak of a clean gold standard sample was about 1.6 eV. A flood gun set at 8 eV and a Ni grid placed 3 mm above the sample surface were used for charge stabilisation.[38] The C-(C,H) component of the C1s peak of carbon has been fixed to 284.8 eV to set the binding energy scale. Data treatment was performed with the CasaXPS program (Casa Software Ltd, UK, version 2.3.16), some spectra were decomposed with the least squares fitting routine provided by the software with a Gaussian/Lorentzian (85/15) product function and after subtraction of a non linear baseline.[39] Molar fractions were calculated using peak areas normalised on the basis of acquisition parameters and sensitivity factors provided by the manufacturer.

Silver nanoparticles are characterized with a Philips CM100 TEM. Typically, the Pox(mDOPA)-Ag^0 solution is diluted 10 times before analysis. A drop of the as-prepared suspension is put onto a carbon-coated Cu grid coated by a Formvar film for at least one min and then lyophilized in order to fix the system and avoid particle agglomeration. Pox(mDOPA)/PAH and Pox(mDOPA)-Ag^0/PAH nanogels were characterized with the same microscope. The nanogels solution is diluted 10 times before analysis by putting a drop of the as-prepared suspension onto a carbon-coated Cu grid coated by a Formvar film for at least one min and then lyophilized.

A Delsa Nano C Particle Analizer (Beckman Coulter) equipped with a laser diode source (wavelength 658 nm; power 30 mW) is used for measuring the hydrodynamic diameter of the aqueous nanogels solutions. Scattering data are collected for at least 70 individual measurements at a constant scattering angle and averaged for each sample. The obtained scattering data are fitted using a volume-weighted cumulative analysis to estimate the diffusion coefficient of the nanogels in solution. The hydrodynamic diameter of the samples (D_H) is obtained using Stokes-Einstein relationship.

^{13}C CP MAS NMR spectra were recorded with 4 mm zirconia rotors spinning at 10 kHz on a Bruker Avance DSX 400WB spectrometer (B0 = 9.04 T) working at Larmor frequency of 100.6 MHz. Cross polarization experiments were performed with a delay time of 5 s and a contact of 2 ms.

Acoustic intermittent contact mode AFM measurements are performed in air at room temperature using a PicoPlus 5500 microscope (Agilent Technologies, Inc.) and Silicon cantilevers (PPP-NCH, Nanosensors; nominal spring constant 42 N/m). Gwyddion SPM data analysis software is used to analyze the data.

Durability Assessments: Immersion test: Stainless steel coated substrates are dipped in 10 mL of water, fatty alcohol ethoxylates based household cleaner diluted ten times at pH around 7.4 (diluted hhc), or NaOH 0.1M for one night at room temperature or at 50 °C.

Mechanical test: Stainless steel coated substrates are cleaned with a sponge wet with distilled water by 25 back and forth movements on each face after an immersion in hot water (10 mL) for one night.

Antibacterial Assessment: The antibacterial activity of the films deposited onto stainless steel against the Gram-negative bacteria *Escherichia coli* is assessed by a viable cell-counting method.[18] A preculture of *E. coli* (Migula 1895) is used to seed a fresh culture into nutrient broth LB (100 mL) and the bacterial culture is incubated at 37 °C for 4 h. At this stage, the culture of *E. coli* contained ca. 10^8 cells mL^{-1} (absorbance at 600 nm equal to 0.6) and is used for the test. The original cell concentration is determined by the spread plate method. Upon appropriate dilution with sterilized 0.9% saline solution, a culture of about 10^5 cells mL^{-1} is prepared and used for antibacterial testing. Films deposited onto 2 × 2 cm SS coupons are sterilized by UV irradiation (15 min for each face) and exposed to the *E. coli* cell suspension (15 mL containing about 10^5 cells mL^{-1}). At a specified time, the bacteria culture (0.1 mL) is added to sterilized 0.9% saline solution (0.9 mL) (the solution was sterilized at 121 °C for 20 min), and several dilutions are carried out. The surviving bacteria are counted by the spread-plate method. At various exposure times, 0.1 mL portions are removed and quickly spread on the nutrient agar. After inoculation, the plates are incubated at 37 °C for 24 h, and the colonies are counted. The same procedure was followed for the antibacterial assessments against *S. epidermidis*.

In Vitro Antiadhesion Test: A preculture of *Staphylococcus epidermidis* ATCC35984 or *Escherichia coli* ATCC47076 was grown overnight at 37 °C in LB (3 mL) and used the next morning to seed a fresh culture in LB (50 mL). The bacterial concentration of test inoculum was adjusted to about 10^8–10^9 cells mL^{-1} in LB.

Stainless steel coupons coated with anti-adhesive films were placed in Petri dishes containing damp blotting paper. Test inoculum (200 µL) was pipetted onto each substrate. The Petri dishes containing the inoculated coupons were closed and incubated at 37 °C for 18 h.

The stainless steel substrates were rinsed twice with sterile deionized water (10 mL) to remove non-adherent bacteria, and then placed face downward in glass jars containing 500-fold-diluted LB (20 mL) and 4-mm glass beads. The jars were shaken horizontally for 10 min and then their contents were sonicated in a water bath (50–60 KHz) for 2 min. Viable bacteria were counted by plating 10-fold dilutions on LB agar. The plates were incubated at 37 °C overnight and for an additional 72 h at room temperature before colony-forming units were counted. Reported results are averages of at least 3 replicates.

Biofilm Formation Assessment: A preculture of *Staphylococcus epidermidis* ATCC35984 or *Escherichia coli* ATCC47076 was grown overnight at 37 °C in LB (3 mL) and used the next morning to seed a fresh culture in LB (50 mL). The bacterial concentration of test inoculum was adjusted to about 10^7–10^8 cells mL^{-1} in M63 medium (pH 5.9) supplemented with glucose and casamino acids.

Stainless steel coupons coated with DspB films were placed in Petri dishes containing damp blotting paper. Test inoculum (200 µL) was pipetted onto each substrate. The Petri dishes containing the inoculated coupons were closed and incubated at 37 °C for 24 h.

Viable Bacteria Counts: The stainless steel substrates were rinsed twice with sterile DI water (10 mL) to remove non-adherent bacteria, and then placed face downward in glass jars containing 500-fold-diluted LB (20 mL) and 4-mm glass beads. The jars were shaken horizontally for 10 min, and then their contents were sonicated in a water bath (50–60 KHz) for 2 min. Viable bacteria were counted by plating 10-fold dilutions on LB agar. The plates were incubated at 37 °C overnight before colony-forming units were counted. Finally, in order to demonstrate that all bacteria were removed from the plate, each substrate was rinsed twice with sterile deionized water (10 mL) and then laid onto LB agar containing 2,3,5-triphenyltetrazolium chloride dye (25 mg L^{-1}; Fluka, ref. 93140). After 24 to 72-h incubation at 37 °C,

strongly adherent live bacteria remaining on the samples appeared as purple CFU and were counted. All colony counts results are averages of at least 3 replicates.

Fluorescent Microscopic Visualization: Biofilm was visualized directly on the stainless steel coupons by labeling bacteria with a solution of two fluorochromes: propidium iodide (final concentration 8.1 µM) and SYTO 9 (final concentration 63 nM). After incubation for 15 min at 22 °C ± 2 °C in the dark and removal of the inoculum in excess, biofilm was observed with an epifluorescence microscope (Olympus BX60/U-RFL-T, oil immersion, 1000× magnification). Cells that fluoresced green had intact membranes whereas cells that fluoresced red had compromised membranes. Adherent cells were motionless whereas non-adhering ones were in motion.

Supporting Information

Supporting Information is available from the Wiley Online Library or from the author.

Acknowledgements

E.F. and C.F.-D. contributed equally to this work. The research was partly supported by BELSPO (IUAP VI/27), the Walloon Region (PPP program BIOCOAT), the University of Liège and the National funds for Scientific Research (FRS-FNRS). The authors thank the BIOCOAT team members for their contribution, in particular H. Vandegaardt, C. De Bona, A. Wislez, and F. Farina.

Received: April 20, 2012
Revised: June 26, 2012
Published online: August 9, 2012

[1] a) G. Decher, J. D. Hong, *Makromol. Chem.-Macromol. Symp.* **1991**, *46*, 321; b) G. Decher, *Science* **1997**, *277*, 1232.
[2] a) P. T. Hammond, *Curr. Opin. Colloid Interface Sci.* **2000**, *4*, 430; b) S. A. Sukhishvili, *Curr. Opin. Colloid Interface Sci.* **2005**, *10*, 37.
[3] a) E. Kharlampieva, S. A. Sukhishvili, *Polym. Rev.* **2006**, *46*, 377; b) E. Kharlampieva, V. Kozlovskaya, S. A. Sukhishvili, *Adv. Mater.* **2009**, *21*, 3053.
[4] a) J. F. Quinn, A. P. R. Johnston, G. K. Such, A. N. Zelikin, F. Caruso, *Chem. Soc. Rev.* **2007**, *36*, 707; b) D. E. Bergbreiter, K.-S. Liao, *Soft Matter* **2009**, *5*, 23.
[5] a) J. Sun, T. Wu, Y. Sun, Z. Wang, Z. Xi, J. Shen, W. Cao, *Chem. Commun.* **1998**, 1853; b) J. Chen, L. Huang, L. Ying, G. Luo, X. Zhao, W. Cao, *Langmuir* **1999**, *15*, 7208; c) I. Pastoriza-Santos, B. Scholer, F. Caruso, *Adv. Funct. Mater.* **2001**, *11*, 122; d) S. Qin, D. Qin, W. T. Ford, Y. Zhang, N. A. Kotov, *Chem. Mater.* **2005**, *17*, 2131.
[6] a) J. J. Harris, P. M. DeRose, M. L. Bruening, *J. Am. Chem. Soc.* **1999**, *121*, 1978; b) J. Dai, D. M. Sullivan, M. L. Bruening, *Ind. Eng. Chem. Res.* **2000**, *39*, 3528; c) S. Y. Yang, M. F. Rubner, *J. Am. Chem. Soc.* **2002**, *124*, 2100; d) F. Mallwitz, A. Laschewsky, *Adv. Mater.* **2005**, *17*, 1296.
[7] a) T. Serizawa, K. Nanameki, K. Yamamoto, M. Akashi, *Macromolecules* **2002**, *35*, 2184; b) V. Kozlovskaya, S. Ok, A. Sousa, M. Libera, S. A. Sukhishvili, *Macromolecules* **2003**, *36*, 8590; c) T. Serizawa, Y. Nakashima, M. Akashi, *Macromolecules* **2003**, *36*, 2072; d) T. Serizawa, D. Matsukuma, K. Nanameki, M. Uemura, F. Kurusu, M. Akashi, *Macromolecules* **2004**, *37*, 6531; e) A. Schneider, C. Vodouhe, L. Richert, G. Francius, E. Le Guen, P. Schaaf, J.-C. Voegel, B. Frisch, C. Picart, *Biomacromolecules* **2007**, *8*, 139; f) T. Boudou, T. Crouzier, R. Auzely-Velty, K. Glinel, C. Picart, *Langmuir* **2009**, *25*, 13809; g) N. Nuraje, R. Asmatulu, R. E. Cohen, M. F. Rubner, *Langmuir* **2011**, *27*, 782.
[8] Z. Lu, C. M. Li, Q. Zhou, Q.-L. Bao, X. Cui, *J. Colloid Interface Sci.* **2007**, *314*, 80.
[9] E. S. Dragan, F. Bucatariu, *Macromol. Rapid Commun.* **2010**, *31*, 317.
[10] a) G. K. Such, J. F. Quinn, A. Quinn, E. Tjipto, F. Caruso, *J. Am. Chem. Soc.* **2006**, *128*, 9318; b) D. E. Bergbreiter, B. S. Chance, *Macromolecules* **2007**, *40*, 5337; c) G. K. Such, E. Tjipto, A. Postma, A. P. R. Johnston, F. Caruso, *Nano Lett.* **2007**, *7*, 1706.
[11] a) Y. Ma, L. Qian, H. Huang, X. Yang, *J. Colloid Interface Sci.* **2006**, *295*, 583; b) W. Tong, C. Gao, H. Mohwald, *Macromol. Rapid Commun.* **2006**, *27*, 2078; c) H. Lee, S. M. Dellatore, W. M. Miller, P. B. Messersmith, *Science* **2007**, *318*, 426.
[12] a) A. Charlot, V. Sciannamea, S. Lenoir, E. Faure, R. Jerome, C. Jerome, C. Van De Weerdt, J. Martial, C. Archambeau, N. Willet, A.-S. Duwez, C.-A. Fustin, C. Detrembleur, *J. Mater. Chem.* **2009**, *19*, 4117; b) C. Falentin-Dandre, E. Faure, T. Svaldo Lanero, F. Farina, C. Jerome, C. Van de Weerdt, J. Martial, A.-S. Duwez, C. Detrembleur, *Langmuir* **2012**, *28*, 7233.
[13] a) J. H. Waite, M. L. Tanzer, *Science* **1981**, *212*, 1038; b) M. Yu, J. Hwang, T. J. Deming, *J. Am. Chem. Soc.* **1999**, *121*, 5825; c) B. P. Lee, P. B. Messersmith, J. N. Israelachvili, J. H. Waite, *Annu. Rev. Mater. Res.* **2011**, *41*, 99.
[14] a) L. A. Burzio, J. H. Waite, *Biochemistry* **2000**, *39*, 11147; b) H. Lee, N. F. Scherer, P. B. Messersmith, *Proc. Natl. Acad. Sci. USA* **2006**, *103*, 12999; c) H. O. Ham, Z. Liu, K. H. A. Lau, H. Lee, P. B. Messersmith, *Angew. Chem. Int. Ed.* **2011**, *50*, 732.
[15] E. Faure, P. Lecomte, S. Lenoir, C. Vreuls, C. Van De Weerdt, C. Archambeau, J. Martial, C. Jerome, A.-S. Duwez, C. Detrembleur, *J. Mater. Chem.* **2011**, *21*, 7901.
[16] H. Lee, Y. Lee, A. R. Statz, J. Rho, T. G. Park, P. B. Messersmith, *Adv. Mater.* **2008**, *20*, 1619.
[17] D. Lee, R. E. Cohen, M. F. Rubner, *Langmuir* **2005**, *21*, 9651.
[18] a) T. J. Franklin, *Biochemistry of Antimicrobial Action*, 3rd ed., Chapman & Hell, London **1981**; b) A. Kanazawa, T. Ikeda, T. Endo, *J. Polym. Sci. Part A: Polym. Chem.* **1993**, *31*, 3031.
[19] G. B. Sukhorukov, H. Moehwald, G. Decher, Y. M. Lvov, *Thin Solid Films* **1996**, *284–285*, 220.
[20] K. A. Marx, *Biomacromolecules* **2003**, *4*, 1099.
[21] a) P. Gilbert, A. J. McBain, A. H. Rickard, *Int. Biodeterior. Biodegrad.* **2003**, *51*, 245; b) T.-F. C. Mah, G. A. O'Toole, *Trends Microbiol.* **2001**, *9*, 34.
[22] A. Statz, J. Finlay, J. Dalsin, M. Callow, J. A. Callow, P. B. Messersmith, *Biofouling* **2006**, *22*, 391.
[23] G. Cheng, Z. Zhang, S. Chen, J. D. Bryers, S. Jiang, *Biomaterials* **2007**, *28*, 4192.
[24] S. M. Olsen, L. T. Pedersen, M. H. Laursen, S. Kiil, K. Dam-Johansen, *Biofouling* **2007**, *23*, 369.
[25] I. Banerjee, R. C. Pangule, R. S. Kane, *Adv. Mater.* **2011**, *23*, 690.
[26] S. Gabriel, P. Dubruel, E. Schacht, A. M. Jonas, B. Gilbert, R. Jerome, C. Jerome, *Angew. Chem. Int. Ed.* **2005**, *44*, 5505.
[27] a) K. L. Prime, G. M. Whitesides, *Science* **1991**, *252*, 1164; b) K. L. Prime, G. M. Whitesides, *J. Am. Chem. Soc.* **1993**, *115*, 10714.
[28] a) L. Ionov, A. Synytska, E. Kaul, S. Diez, *Biomacromolecules* **2010**, *11*, 233; b) N.-P. Huang, R. Michel, J. Voros, M. Textor, R. Hofer, A. Rossi, D. L. Elbert, J. A. Hubbell, N. D. Spencer, *Langmuir* **2001**, *17*, 489; c) J. P. Bearinger, S. Terrettaz, R. Michel, N. Tirelli, H. Vogel, M. Textor, J. A. Hubbell, *Nat. Mater.* **2003**, *2*, 259.
[29] a) N. Xia, Y. Hu, D. W. Grainger, D. G. Castner, *Langmuir* **2002**, *18*, 3255; b) D. Bozukova, C. Pagnoulle, M.-C. De Pauw-Gillet, S. Desbief, R. Lazzaroni, N. Ruth, R. Jerome, C. Jerome, *Biomacromolecules* **2007**, *8*, 2379.

[30] a) K. Glinel, A. M. Jonas, T. Jouenne, J. Leprince, L. Galas, W. T. S. Huck, *Bioconjugate Chem.* **2009**, *20*, 71; b) X. Laloyaux, E. Fautre, T. Blin, V. Purohit, J. Leprince, T. Jouenne, M. Jonas Alain, K. Glinel, *Adv. Mater.* **2010**, *22*, 5024.
[31] N. Ramasubbu, L. M. Thomas, C. Ragunath, J. B. Kaplan, *J. Mol. Biol.* **2005**, *349*, 475.
[32] Y. Itoh, X. Wang, B. J. Hinnebusch, J. F. Preston, T. Romeo, *J. Bacteriol.* **2005**, *187*, 382.
[33] J. B. Kaplan, C. Ragunath, K. Velliyagounder, D. H. Fine, N. Ramasubbu, *Antimicrob. Agents Chemother.* **2004**, *48*, 2633.
[34] G. Donelli, I. Francolini, D. Romoli, E. Guaglianone, A. Piozzi, C. Ragunath, J. B. Kaplan, *Antimicrob. Agents Chemother.* **2007**, *51*, 2733.
[35] a) A. Caro, V. Humblot, C. Methivier, M. Minier, M. Salmain, C. M. Pradier, *J. Phys. Chem. B* **2009**, *113*, 2101; b) S. Yuan, D. Wan, B. Liang, S. O. Pehkonen, Y. P. Ting, K. G. Neoh, E. T. Kang, *Langmuir* **2011**, *27*, 2761; c) M. Minier, M. Salmain, N. Yacoubi, L. Barbes, C. Methivier, S. Zanna, C. M. Pradier, *Langmuir* **2005**, *21*, 5957; d) A. Caro, V. Humblot, C. Methivier, M. Minier, L. Barbes, J. Li, M. Salmain, C. M. Pradier, *J. Colloid Interface Sci.* **2010**, *349*, 13.
[36] a) M. J. LaVoie, B. L. Ostaszewski, A. Weihofen, M. G. Schlossmacher, D. J. Selkoe, *Nat. Med.* **2005**, *11*, 1214; b) H. Lee, J. Rho, P. B. Messersmith, *Adv. Mater.* **2009**, *21*, 431; c) L. Q. Xu, W. J. Yang, K.-G. Neoh, E.-T. Kang, G. D. Fu, *Macromolecules* **2010**, *43*, 8336.
[37] A. Caro, V. Humblot, C. Methivier, M. Minier, L. Barbes, J. Li, M. Salmain, C.-M. Pradier, *J. Colloid Interface Sci.* **2010**, *349*, 13.
[38] C. E. Bryson III, *Surf. Sci.* **1987**, *189–190*, 50.
[39] D. A. Shirley, *Phys. Rev. B* **1972**, *5*, 4709.